HHS Public Access

Author manuscript

Nat Biotechnol. Author manuscript; available in PMC 2012 June 01.

Published in final edited form as:

Nat Biotechnol. ; 29(10): 934–941. doi:10.1038/nbt.1972.

CD140a identifies a population of highly myelinogenic, migration-competent, and efficiently engrafting human oligodendrocyte progenitor cells

Fraser J. Sim[1,2,3], **Crystal McClain**[1], **Steven Schanz**[1], **Tricia L. Protack**[1], **Martha S. Windrem**[1], and **Steven A. Goldman**[1,2]

[1]Dept. of Neurology, University of Rochester Medical Center, Rochester, NY 14642

[2]Dept. of Neurosurgery, University of Rochester Medical Center, Rochester, NY 14642

[3]Dept. of Pharmacology, State Univ. New York at Buffalo, Buffalo, NY 14214

Abstract

Experimental models of myelin disorders can be treated by the transplantation of oligodendrocyte progenitor cells (OPCs) into the affected brain or spinal cord. OPCs express gangliosides recognized by MAb A2B5, but this marker also identifies lineage-restricted astrocytes and immature neurons. To establish a more efficient means of isolating myelinogenic OPCs, we asked if FACS could be used to sort PDGFα receptor+ cells from fetal human forebrain, based on expression of the PDGFRα epitope CD140a. CD140a+ isolates were maintained as mitotic bipotential progenitors that could be instructed to either oligodendrocyte or astrocyte fate. Transplanted CD140a+ cells were highly migratory, and rapidly and robustly myelinated the hypomyelinated shiverer mouse brain, more efficiently than did A2B5-sorted cells. Microarray analysis of CD140a+ cells revealed their differential expression of CD9, as well as of PTN-PTPRZ1, wnt, notch and BMP pathway components, indicating the dynamic interaction of self-renewal and fate-restricting pathways in these cells.

Keywords

oligodendrocyte progenitor; PDGF receptor; myelin; remyelination

Disorders of myelin are among the most prevalent and diverse neurological disorders. They include conditions as diverse as the childhood hereditary leukodystrophies, cerebral palsy, subcortical stroke, multiple sclerosis, and vascular white matter disease, among others[1–3].

Address correspondence to either: Fraser Sim, Ph.D., fjsim@buffalo.edu, or Dr. Steve Goldman, Dept. of Neurology, University of Rochester Medical Center, 601 Elmwood Rd., Box 645, Rochester, NY 14642, 585-275-9550, Steven_Goldman@urmc.rochester.edu.

Author contributions

FJS directed both the in vitro experiments and genomics analysis; CM planned and performed the in vitro studies with FJS, and conducted the assessment of OPC ontogeny; SS performed the transplants of $A2B5^+$ and $CD140^+$ cells into shiverer mice; TP assisted FJS and CM in the in vitro studies and FACS analysis; MSW directed the comparative assessment of myelination by A2B5 and CD140 cells in vivo; SAG co-designed the experiments, co-analyzed the data with FJS and MW, and wrote the paper together with the co-authors.

These conditions have in common the loss of central oligodendrocytes, the sole myelin-producing cell of the brain and spinal cord, and each requires oligodendrocytic replacement and remyelination as an antecedent to recovery. Myelinogenic oligodendrocyte progenitor cells pervade the parenchyma of both the developing and adult human brain[4–6], and we have developed strategies for their isolation and transplantation, by which we have established the ability of these cells to efficiently remyelinate the dysmyelinated brain and spinal cord [7–9]. However, we have hitherto isolated these cells on the basis of their expression of gangliosides recognized by monoclonal antibody (MAb) A2B5 [5, 10–12], the targets of which are expressed by multiple phenotypes besides oligodendrocyte progenitors. In particular, developing neurons also express A2B5, necessitating their exclusion from A2B5-sorted isolates derived from fetal human brain tissue. We thus used PSA-NCAM-based depletion of neuronal progenitors, prior to A2B5-based immunoselection, to prepare enriched populations of OPCs from fetal human brain tissue, which proved able to myelinate and ultimately rescue the congenitally hypomyelinated shiverer mouse[7, 9]. Yet these studies also revealed that fetal A2B5-defined OPCs were still phenotypically heterogeneous, and included a large fraction of non-myelinogenic cells restricted to astrocytic fate. To more precisely enrich myelinogenic OPCs, we thus sought to identify better markers for their definitive isolation. To this end, we asked if genes already recognized as selectively expressed by adult human OPCs, which are highly biased to oligodendrocyte fate, might serve as markers by which to isolate oligodendrocyte-biased OPCs from the fetal brain as well. In this regard, we had previously found that human A2B5$^+$ oligodendrocyte progenitors highly over-express mRNAs encoding both the NG2 chondroitin sulfate proteoglycan, and PDGFRA, the platelet derived growth factor-α receptor[13], suggesting the utility of each as potentially more efficient at isolating oligodendrocyte-biased OPCs[14, 15]. While NG2 is also expressed by pericytes, which limited its utility as a selection marker, PDGFRα appears to be expressed specifically by OPCs in both rodents [16–18] and humans[6, 13, 19, 20].

Yet despite the potential attraction of a PDGFαR-based immunoselection strategy, no one had ever enriched OPCs using that's strategy. In part, this failure was due to the incompatibility of standard dissociation techniques with PDGFαR-based immunoselection. To address these issues, we thus paired the use of an antibody against CD140a, which recognizes a human PDGFRα-ectodomain, with a compatible papain-based dissociation procedure[7], to isolate CD140a$^+$/PDGFRα$^+$ OPCs from the fetal human brain. We confirmed that these cells were able to give rise to both oligodendrocytes and astrocytes, in a BMP and serum-dependent fashion, and that their oligodendrocytic progeny could robustly myelinate the hypomyelinated shiverer mouse brain. Importantly, CD140a$^+$ cells exhibited more rapid and efficient myelination than did their A2B5$^+$/PSA-NCAM$^-$ counterparts. In addition, expression profiling confirmed that CD140a$^+$ cells differentially express transcripts characteristic of oligodendroglial progenitors. These differentially expressed genes encoded surface antigens such as CD9[21, 22], thereby identifying alternative ectodomains by which to sort OPCs, as well as components of the wnt and notch pathways, which may be critical to the turnover and fate of fetal human OPCs.

RESULTS

CD140a defines a population of olig2$^+$ glial progenitor cells

In the human forebrain, OPCs are most actively generated during the second trimester. To assess the geographic distribution of CD140a/PDGFRα$^+$ cells during that period, we immunolabeled sections of 22 week g.a. forebrain with monoclonal anti-CD140a IgG, which recognizes a PDGFRα ectodomain[23]. Immunostaining revealed that CD140a$^+$ cells pervaded the forebrain, extending through the intermediate zone to the developing cortical mantle (Fig. 1A), with a morphology similar to that of NG2-defined adult OPCs[24], and a distribution which anticipated that observed in the adult human forebrain[4–6]. Virtually all CD140a$^+$ cells co-expressed the oligodendrocyte lineage transcription factor olig2 (Fig. 1B), while sox2 was co-expressed by a fraction (Fig. 1C). A significant proportion of CD140a$^+$ cells expressed Ki67, a marker of actively cycling cells (Fig. 1D). In contrast, no co-localization of CD140a-immuno-reactivity was noted with either astrocytic glial fibrillary acidic protein (GFAP) or neuronal Hu protein. Together, these data suggest that CD140a$^+$ cells comprise a pool of uncommitted OPCs that ubiquitously co-express olig2.

CD140a$^+$ cells appeared and accumulated during second trimester cortical expansion

Flow cytometry revealed an abundant population of CD140a$^+$/PDGFRα$^+$ cells at 20–22 weeks gestation, by which point 4.8 ± 0.7% of cells within cortical dissociates, which included admixed intermediate zone and cortical mantle, were sorted as CD140a$^+$ (n=13, standard error [SE]). (Fig. 2A/B). At earlier gestational ages however, relatively few CD140a$^+$ cells were noted; appreciable numbers first began to appear in forebrain dissociates at 16 weeks g.a.. Over the period of 16–23 weeks, we noted a significant correlation between the incidence of cortical CD140a$^+$ cells and gestational age ($p<0.0001$, $r^2=0.43$, df = 26) (Fig. 2C). In contrast, the relative incidence of CD140a$^+$ cells within the dissected ventricular and subventricular zones (VZ/SVZ) did not increase with gestational age ($p=0.57$, $r^2=0.04$, df = 10) (Fig. 2D). The relatively constant proportion of CD140a$^+$ cells in the VZ/SVZ, in contrast to the rapidly increasing proportion of CD140a$^+$ cells in cortical dissociates (3.1 ± 0.4 vs. 1.2 ± 0.1%; unpaired t-test, $p=0.012$, df=37), suggested a monotonic colonization of the developing brain by newly generated VZ/SVZ-derived OPCs (Fig. 2E).

CD140a$^+$/PDGFRα$^+$ cells comprise a subpopulation of A2B5$^+$ glial progenitor cells

A2B5$^+$/PSA-NCAM$^-$ cells derived from the fetal human brain comprise a phenotypically heterogeneous cell population. Although these cells include a myelinogenic fraction of bipotential OPCs[7, 9], they also include a GFAP$^+$ fraction that appear restricted to astrocyte phenotype. We thus asked if CD140a$^+$/PDGFRα$^+$ OPCs comprised a discrete fraction of the A2B5$^+$/PSA-NCAM$^-$ population. Dissociated fetal cells were first depleted of PSA-NCAM$^+$ cells by immunomagnetic sorting, and then subjected to two-color flow cytometry for A2B5 and CD140a (Fig. 3A–C). We found that CD140a$^+$ cells were significantly more abundant in the A2B5$^+$/PSA-NCAM$^-$ pool than in the unsorted population from which both derived (23.2 ± 3% in A2B5$^+$/PSA-NCAM$^-$ vs. 10.9 ± 3% in the initial dissociate; t-test $p=0.0324$, n=4) (Fig. 3D).

These data indicated that CD140a$^+$ cells comprised a subpopulation of A2B5$^+$ OPCs. On that basis, we next asked whether the oligodendrocyte-competent fraction of glial progenitors was specifically enriched in the CD140a subpopulation. To this end, A2B5$^+$/PSA-NCAM$^-$ and CD140a$^+$ cells derived in parallel from the same tissue samples (n=3) were plated into base media supplemented with 1% platelet-depleted serum (PD-FBS) and triiodothyronine (T3; 30 ng/ml), to assess their potential to differentiate as oligodendrocytes (n=3 samples, each done in triplicate wells/phenotype). After 7 days, matched cultures were immunostained using MAb O4, which recognizes immature post-mitotic oligodendrocytes in humans[5, 25, 26]. We found that the proportion of O4$^+$ oligodendrocytes was substantially greater in all CD140a$^+$ fractions than in their CD140a$^-$ counterparts (n=3 sorts) (Fig. 3E).

Oligodendrocyte generation was restricted to CD140a$^+$ cells

Since only a fraction of A2B5$^+$ cells generate oligodendrocytes[7], and since only some A2B5$^+$ cells co-express CD140a, we next asked if oligodendrocytes arose *exclusively* from the CD140a$^+$ subpopulation. To this end, we used fluorescence-activated cell sorting (FACS) to separately isolate CD140a$^+$ and CD140$^-$ cells. Immediately after sorting, the CD140a$^+$ cells were found to be uniform in size, relatively small and phase bright. Within 24 hrs, most were observed to elaborate fine processes, initially as bipolar cells (Supplemental Fig. 1A). These cells uniformly expressed CD140a/PDGFRα (Supplemental Figs. 1B–C), and co-expressed the transcription factors olig2 and sox2, which are both expressed by uncommitted glial progenitors (Supplemental Figs. 1D–E). In contrast, the CD140a$^-$ fraction was largely devoid of olig2$^+$ cells (Supplemental Fig. 1F). The vast majority of CD140a$^-$ cells exhibited a neuronal phenotype, expressing both βIII-tubulin and the neuronal mRNA binding protein Hu (Supplemental Fig. 1G). In addition, a subpopulation of cells in the CD140a$^-$ fraction also expressed astrocytic markers, including both GFAP and aquaporin 4 (Supplemental Fig. 1H).

To promote oligodendrocytic differentiation, the two populations were then each raised in T3-supplemented media. Within 1–2 days, most CD140a$^+$ cells exhibited a bipolar progenitor morphology and expressed nuclear olig2. After 4 days, 36.6 ± 5% of CD140a-sorted cells expressed the oligodendrocytic sulfatide recognized by MAb O4 (n=13) (Fig. 4A), whereas <0.1% of CD140a$^-$ cells expressed O4-immunoreactivity at this point (n=7) (Fig. 4B). CD140a-derived O4$^+$ cells matured as O1$^+$ and MBP$^+$ oligodendrocytes by 7 days *in vitro* (Fig. 4C). In contrast, at 7 days the vast majority of CD140a$^-$ cells were either βIIItubulin$^+$ neurons (63 ± 8%, n=4 samples), or GFAP$^+$ astrocytes (6 ± 2%, n=4) (Fig. 4D). A subset of A2B5$^+$ cells (21 ± 1%, n=3), some of which co-expressed GFAP, was also noted in CD140a$^-$ cultures. Nonetheless, neither exposure to serum concentrations up to 10%, nor supplementation by 20 ng/ml IGF1, triggered the appearance of O4$^+$ oligodendrocytes in CD140a$^-$ cultures. Overall, we noted a >200-fold increase in the percentage of O4$^+$ cells arising from CD140a$^+$ cells, relative to their CD140a$^-$ counterparts (37% CD140a$^+$ vs. 0.14% CD140a$^-$, $p<0.0001$, two-tailed t-test; df=18). Thus, O4$^+$ oligodendrocytes were produced only by CD140a$^+$ progenitor cells.

CD140a$^+$ cells can be instructed to generate both oligodendrocytes and astrocytes

Since oligodendrocytic fate potential was restricted to CD140a$^+$ cells, we next asked if CD140a$^+$ cells could also be induced to astrocytic fate, using serum or BMP exposure, as previously noted in adult-derived OPCs[13]. We found that addition of either serum or BMP-4 after FACS induced rapid GFAP$^+$ astrocytic differentiation. Within 7 days of post-sort exposure to 0.5% PD-FBS, cultures exhibited a >3.5-fold rise in GFAP$^+$ astrocytes, from 8.8% to 30.7% ($p=0.002$, unpaired t-test, df=5). Similarly BMP-4 exposure (50 ng/ml) yielded a dose-dependent increase in astrocytes, from 8% to >40% at 4 days ($p<0.01$; $F = 12.4$; ANOVA with Dunnett's post hoc analysis). In contrast, oligodendrocyte differentiation was inhibited by BMP-4; O4$^+$ cells declined from >30% to <5% at 4 days ($p<0.01$; $F = 12.7$). As a result, the GFAP/O4 ratio in these cultures increased in response to BMP-4, from <0.5 to > 15.

Importantly, CD140a$^+$ cells could be maintained as bipotential progenitors in vitro. PDGF-AA and FGF2 (each 20 ng/ml) inhibited oligodendrocytic differentiation, such that only 2.4 ± 1.2% and 4.8 ± 1.3 of PDGF-AA/FGF2-exposed CD140a$^+$ cells developed O4 immuno-reactivity by days 4 and 7 (n=5); under these conditions, most cells remained as A2B5$^+$ progenitors (75 ± 7%, n=6), accompanied by the gradual appearance of GFAP$^+$ astrocytes (8.8± 1.9%, n=4). Importantly, FGF2 withdrawal and addition of T3 favored oligodendrocyte differentiation, increasing the incidence of O4$^+$ cells to 13.7 ± 2.9 % ($p=0.01$, t-test; n=3). In addition, astrocyte lineage commitment could be blocked by noggin, a soluble competitive antagonist of the BMPs. When added to CD140a$^+$ cells in the absence of growth factors for 4 days, 100 ng/ml noggin potently inhibited BMP4-induced astrocytic differentiation ($p<0.05$, Tukey's post hoc test), and was also sufficient to reverse the inhibitory effect of BMP-4 on oligodendrocyte commitment (21.0 ± 3% O4$^+$ cells in BMP-4 + noggin, vs. 4.3 ± 1% O4$^+$ cells in BMP-4 alone; $p<0.05$). Interestingly, baseline levels of astrocytic and oligodendrocytic differentiation (8.1 ± 3% and 22.6 ± 4%, respectively) were unaffected by 100 ng/ml noggin in the absence of exogenous BMP (8.1 ± 4% GFAP$^+$ and 21.0 ± 3% O4$^+$).

CD140a$^+$ OPCs myelinated the hypomyelinated shiverer mouse brain upon xenograft

We next asked if CD140a-sorted cells could differentiate as mature oligodendrocytes *in vivo* as well as *in vitro*, and whether their derived oligodendrocytes were competent to myelinate axons *in vivo*. To this end, we transplanted 10 neonatal myelin-deficient shiverer$^{shi/shi}$ mice with 5×10^4 cells each of CD140a-sorted OPCs. The xenografts were delivered shortly after birth as intracallosal injections, as previously described[7]. Under these conditions, A2B5$^+$/PSA-NCAM$^-$ sorted fetal human OPCs typically begin to generate myelin by 8 weeks after transplant, myelinating relatively large volumes of otherwise hypomyelinated white matter by 12 weeks[7]. To assess the relative competence of CD140a-sorted cells to effect myelin production and axonal ensheathment, the CD140a-engrafted shiverers were sacrificed at either 8 (n=7) or 12 (n=3) weeks of age, and their brains cryosectioned and immunostained for myelin basic protein (MBP), which is not otherwise expressed in *shiverer*. By 8 weeks, the CD140a-engrafted mice indeed exhibited significant and widespread forebrain myelination, in a distribution similar to but generally broader than that which we had observed using A2B5-sorted OPCs (Figs. 5 and 6A). Quantification within the fimbria

revealed that at 8 weeks after injection, a time-point at which myelinogenesis from implanted A2B5-sorted fetal human OPCs is just beginning (Windrem et al., 2004), 8 ± 3% of CD140-sorted cells had already differentiated as MBP^+ oligodendrocytes (n=3, Figs. 5A, D). At that time-point, the majority of human cells were of oligodendrocytic lineage, such that 68 ± 14% of human nuclear antigen $(hNA)^+$ cells co-expressed olig2, while <5% of human $CD140a^+$ cells had differentiated as $GFAP^+$ astrocytes (Fig. 5C, D). In addition, a third persisted as $NG2^+$ OPCs (31 ± 14%; Fig. 5B, D); a fraction of these remained mitotically competent, as defined by Ki67 (8 ± 4%, n=3; Fig. 5D).

We next compared the performance at 12 weeks of $CD140a^+$ cells, in terms of both their migration and myelination competence, to that of $A2B5^+$/PSA-$NCAM^-$ cells whose in vivo myelination competence we had previously described at that time point. To this end, we assessed the efficiency of callosal axonal ensheathment by $CD140a^+$ cells, using the same transplantation and assessment protocols, source gestational ages, sacrifice time-point and imaging metrics that we had previously described for callosal myelination by fetal $A2B5^+$/PSA-$NCAM^-$ cells (Fig. 6). We found that at 12 weeks, the CD140a-engrafted shiverers exhibited ensheathment of 26.7 ± 2.5% of all callosal axons by human MBP-defined myelin (mean ± SE; n=3 mice) (Figs. 6B–E). Remarkably, in especially dense areas of donor cell engraftment, ensheathment efficiencies approaching 40% were often noted. These data contrasted sharply to the average axonal myelination efficiency by $A2B5^+$/PSA-$NCAM^-$ cells at 12 weeks, of 10.1 ± 2.8% (n=6) (Windrem et al., 2004). Comparing these data sets, the $CD140a^+$ cells myelinated with significantly and substantially higher efficiency at 12 weeks than did their $A2B5^+$/PSA-NCAM- counterparts (Figs. 6E–F) (n=6; $p < 0.01$ by Student's t-test). These results suggested that $CD140a^+$ cells exhibited both a higher efficiency of oligodendrocytic differentiation, and a more rapid initiation of myelinogenesis, than did fetal A2B5-defined OPCs; indeed, the $CD140a^+$ cells myelinated with an efficiency and time course more similar to that which we had previously observed with adult brain-derived $A2B5^+$ OPCs[7]. Unlike adult OPCs, however, fetal $CD140a^+$/$PDGFR\alpha^+$ cells migrated widely, extending as broadly throughout the brain and brainstem as their fetal $A2B5^+$/PSA-$NCAM^-$ counterparts, and with even greater penetration of both cortical and subcortical grey matter (Fig. 6A). Importantly, despite their efficient oligodendrocytic production and myelinogenesis, engrafted $CD140a^+$ cells remained bipotential in vivo, in that they reliably generated astrocytes as well as oligodendrocytes in recipient brains (Fig. 6G–H). Together, these findings indicate that $CD140a^+$ fetal human OPCs exhibit widespread migration and myelinogenesis in vivo, and do so more rapidly and efficiently than the larger pool of $A2B5^+$/PSA-$NCAM^-$ OPCs.

$CD140a^+$ cells express a transcript profile of oligodendrocyte progenitor cells

To better define the differentiation state of $CD140a^+$ human OPCs, we next assessed their expression profiles, relative to $CD140a^-$ cells. We first used Taqman low density arrays to achieve high throughput RT-qPCR of a panel of 48 marker genes, that we chose as potentially predictive of glial cell fate (Table 1). Using 6 fetal cortical samples of 20–22 weeks g.a., sorted on the basis of CD140a, we compared the marker gene expression patterns of the $CD140a^+$ and $CD140a^-$ fractions (Table 1). PDGFRA mRNA was >500 fold higher in $CD140a^+$ than $CD140a^-$ cells (paired t-test, p=0.013), validating both the

stringency of our sorts, and the use of anti-CD140a as a means of isolating PDGFRα$^+$ cells. We also noted significantly higher expression of OPC and oligodendrocyte-lineage markers. For instance, the CSPG4 proteoglycan NG2 was over-expressed almost 50-fold in CD140a$^+$ cells, while the oligodendrocyte lineage transcription factors OLIG2 and SOX10 were expressed >150-fold more in CD140a$^+$ than CD140$^-$ cells. In addition, the progenitor profile of CD140a$^+$/PDGFRα$^+$ cells was confirmed by their significant expression of SOX2[27, 28]. In contrast, neither mature oligodendrocytic genes, such as MBP, PLP MOBP or MOG, nor those selective to astrocytes, such as GFAP or AQP4, were enriched in CD140a$^+$ OPCs (Table 1). Interestingly, while we also noted over-expression of the microglial-selective transcripts CD68 and CD86, migrating human glial progenitors and microglia may share these antigens[29].

Gene expression by CD140a$^+$ OPCs predicts active wnt, notch, and EGF pathways

Using Affymetrix U133+2 arrays, we next compared the transcription profiles of fetal human CD140a-sorted and depleted cells (see Methods). 408 genes were identified as both significantly over-expressed by CD140a$^+$/PDGFRα$^+$ cells (Supplemental Table 1). In accord with our qPCR data, the microarray analysis identified several OPC markers among genes highly expressed by CD140a-sorted cells (Supplemental Table 2). Gene ontology-based and Ingenuity-based pathway analysis identified nervous system development (GO:0007399; $p=8.6 \times 10^{-5}$), neurogenesis ($p=1.6\times10^{-8}$) and, interestingly, schizophrenia ($p=5.0 \times 10^{-12}$). Gene set enrichment analysis (GSEA) identified the WNT, NOTCH, and EGF signaling pathways as over-represented in CD140a-sorted cells ($q = 1.7 \times10^{-3}$, 5.1×10^{-5}, and 9.3×10^{-5}, respectively). CD140a active signaled via WNT as indicated by over-expression of several known WNT target genes (p=0.011) (Supplemental Figure 2). In addition, GSEA of KEGG-defined pathways identified those involved in glycan synthesis as the most differentially regulated by CD140a$^+$ cells (Supplemental Figs. 3A and 3B).

CD9 and PDGFRα are co-expressed in fetal human progenitors

Among membrane proteins, the gene encoding CD9 was 7.4-fold enriched in CD140a$^+$ cells. We thus asked if human OPCs might be further separable using CD9 ectodomain-directed FACS. Flow cytometry revealed that CD9$^+$ cells comprised 2.75 ± 0.7% of all cells in the fetal intermediate zone and cortical plate (n=5), and were less common in the VZ (0.51 ± 0.1%). Two-color cytometry then revealed that the CD9$^+$ pool partially overlapped with that of CD140a$^+$ cells, such that half of CD140a$^+$ OPCs expressed CD9 (49.6 ± 5%, n=6); as such, 2.6 ± 1.5% of the entire dissociated pool co-expressed CD140a and CD9 (Supplemental Figure 4). Indeed, used alone, CD9 based sorting yielded a highly significant, 14-fold enrichment in CD140a$^+$/PDGFRα$^+$ cells relative to their unsorted dissociates (t-test, p=0.00002). These data suggest that CD9 identifies an antigenically distinct subpopulation of OPCs in the fetal human brain, and suggest the utility of concurrent CD9 and CD140a-directed FACS for isolating a highly enriched, oligodendrocyte-competent fraction of human glial progenitor cells.

DISCUSSION

In this study, we developed a CD140a/PDGFRα-based strategy for the direct isolation of OPCs from the fetal human brain. These cells were bipotential for oligodendrocytes and astrocytes, could be instructed to generate one or the other in vitro, and proved robustly myelinogenic in vivo. Importantly, they were even more efficient at in vivo oligodendrocytic differentiation and myelination than were matched isolates of fetal A2B5$^+$/PSA-NCAM$^-$-sorted cells, which comprised the previous standard by which oligodendrocyte progenitors were isolated for therapeutic assessment. In addition, we found that CD140a$^+$ cells expressed a transcriptional profile that manifested the importance of notch, wnt and EGF signaling to both their homeostatic turnover and differentiation. Indeed, their gene expression patterns suggest that fetal human OPCs actively signal to and modulate their local environment, by their robust and selective production of a host of extracellular matrix molecules and secreted ligands.

Our data suggest that in the human forebrain, this process may begin early in the second fetal trimester, with the appearance of the first forebrain OPCs. Indeed, little had previously been known about the ontogeny of OPCs in the human forebrain. PDGFRα and NG2-expressing oligodendrocyte progenitors have been described at 18 weeks g.a. in the developing telencephalon[29, 30], yet we found that CD140a$^+$ cells could be isolated from the fetal brain by 16 weeks g.a., and significantly populated the cortical mantle by 18 weeks g.a. Interestingly, previous studies have noted that O1-defined oligodendrocytes appear at 28–30 weeks g.a. in the human forebrain, coincident with the initial appearance of myelin[30]. Thus, the period spanning 18–30 weeks g.a. appears to comprise the principle period of glial progenitor expansion and oligodendrocytic specification in the developing human forebrain.

We previously noted that fetal human OPCs, when defined as A2B5$^+$/PSA-NCAM$^-$, differentiated as both oligodendrocytes and astrocytes upon neonatal xenograft, and could rescue the otherwise lethal shiverer phenotype[7, 9]. Yet in the present study, we found that not all A2B5$^+$/PSA-NCAM$^-$ cells were CD140/PDGFRα$^+$; rather, CD140a$^+$ cells were enriched within the larger population of A2B5$^+$/PSA-NCAM$^-$ cells. Importantly, *only* CD140a$^+$ cells were capable of oligodendrocyte differentiation in vitro, indicating that CD140a$^+$ cells comprised the entire fraction of A2B5$^+$/PSA-NCAM$^-$ cells responsible for myelination upon xenograft. Thus, our data indicated that the A2B5$^+$/PSA-NCAM$^-$ immunophenotype comprised a heterogeneous pool, that included both astrocyte-restricted CD140a$^-$ cells, and oligodendrocyte-competent CD140a$^+$ progenitors.

The oligodendrocytic bias of fetal human CD140a$^+$ cells was reflected in both their antigenic and gene expression profiles, which were highly enriched in known markers of oligodendroglial lineage (PDGFRA, NG2, ST8SIA1, NKX2.2, OLIG1, OLIG2, and SOX10). Importantly though, human fetal CD140a$^+$/PDGFRα$^+$ cells were not restricted to oligodendrocyte phenotype, but rather were bipotential for astrocytes and oligodendrocytes alike; since when stimulated *in vitro* with serum or BMP4, they readily exhibited astrocytic differentiation. As such, CD140a-sorted fetal human OPCs behave similarly to both their adult human and rodent counterparts, which proliferate in response to PDGF-AA and FGF2[12, 31, 32], and can develop as astrocytes in response to serum or BMPs[13, 33, 34], yet

differentiate as oligodendrocytes when raised in the absence of mitogens or BMPs. As such, CD140a$^+$ cells seem both lineally and phenotypically analogous to bipotential O2A progenitors of the developing rodent brain [7, 33, 34].

The bipotentiality of CD140a$^+$ OPCs is of great practical import: While our data suggest that these cells are superior to fetal A2B5-defined cells in terms of their myelinogenic potential, their differentiated phenotype still depends upon the environment into which they are introduced. Thus, whereas CD140a$^+$ OPCs might be expected to efficiently differentiate as oligodendrocytes and thus effectively remyelinate congenitally hypomyelinated brain, such as in Pelizaeus-Merzbacher disease or cerebral palsy, their use in acute demyelinating disorders, such as in multiple sclerosis or post-ischemic demyelination, might prove to be limited by their astroglial differentiation in an injury environment[35]. Thus, the bilineage competence of these cells must be considered as appropriate clinical targets for their use are further defined.

Although human fetal CD140a$^+$ cells appear bipotential for astrocytes and oligodendrocytes both in vitro and in vivo, we cannot exclude the possibility of discrete CD140a$^+$ subpopulations already restricted to either one phenotype or the other. In particular, it is important to note that even in BMP-stimulated cultures of CD140a$^+$ cells directed to astrocyte phenotype, some oligodendrocytes were noted to develop. This suggested that the CD140a$^+$ pool, while including all OPCs with oligodendrocyte lineage competence, might also include a fraction *restricted* to oligodendrocyte phenotype. We were intrigued then to note the selective expression of mRNA encoding the pro-oligodendroglial tetraspanin CD9[22] by fetal OPCs. Flow cytometry revealed that CD9 was expressed by a discrete subset comprising almost half of all CD140a$^+$ cells, from which the CD9$^+$/CD140a$^+$ fraction could be isolated (Supplemental Figure 4). Interestingly, in development, the pool of CD9-expressing OPCs declines as myelination proceeds[22], suggesting the depletion of a discrete pool of oligodendrocyte-biased progenitors. As such, the CD9$^+$ fraction of CD140a$^+$ OPCs may define an intriguing pool for further assessment as a potential therapeutic vector.

Besides their potential use as transplantable cellular agents for remyelination, OPCs comprise clear targets for therapeutic mobilization and induced differentiation, whether as oligodendrocytes or astrocytes. To better assess the receptors expressed by these cells, and their cognate signaling pathways by which their mobilization and fate are determined, we assessed their patterns of differential gene expression, relative to CD140a- cells. We found that the transcriptional profile of fetal CD140a-defined OPCs largely resembled that of adult A2B5-defined OPCs[13]. Both phenotypes selectively over-expressed a number of chondroitin sulfate proteoglycans, as well as their *cis*-interacting partners. These included the heparin-binding ligand pleiotrophin (PTN), and its principle receptor, protein tyrosine phosphatase-β/ζ (PTPRZ1), a molecule important to both the turnover and fate determination of adult OPCs[13]. One target of PTRPZ1 is β-catenin[36], which may regulate wnt signaling in oligodendroglia[37]. Indeed, this pathway may be regulated differently in fetal than in adult OPCs, as we found significantly higher expression of the wnt transcription factors TCF7L1 and TCF7L2 in fetal CD140a$^+$ cells, than in their A2B5-sorted adult counterparts. These data suggest a possible role for the PTN-PTPRZ1 interaction in regulating wnt signals in fetal human OPCs, differentially so relative to its function in adult human OPCs.

In summary, we have defined a method for the direct, CD140a/PDGFRα-based isolation of a highly myelinogenic pool of OPCs from the fetal human brain, that comprises the entire population of cells capable of rapid oligodendrocyte differentiation. Like A2B5-defined oligodendrocyte progenitors, fetal CD140a$^+$ cells robustly differentiate as myelinating oligodendrocytes when transplanted into the *shiverer* forebrain. Yet unlike the heterogenous population of A2B5-expressing progenitor cells, which includes some but not all oligodendrocyte-competent cells and is also admixed with lineage-restricted fibrous astrocytes, the CD140a-defined pool comprises an exclusive population of cells that uniformly retains oligodendrocytic lineage competence. Importantly, CD140a$^+$ cells differentiate and myelinate more rapidly and efficiently than do fetal A2B5-sorted OPCs, suggesting the potential advantage of CD140a$^+$ cells as cellular vectors for treating disorders of myelin. Indeed, given their relative homogeneity, broad migration competence and rapid myelinogenesis, our data suggest the superiority of CD140a$^+$ cells, relative to previously studied immunophenotypes, as therapeutic reagents for adult as well as pediatric myelin disorders.

MATERIALS AND METHODS

Cell and tissue samples

Fetal brain tissue was obtained from 38 cases (15 – 22 weeks gestational age). Samples were obtained from patients who consented to tissue use under protocols approved by the University of Rochester-Strong Memorial Hospital Research Subjects Review Board. Cortical tissue was dissected into ventricular and sub-ventricular zone and overlying cortical mantle and chilled on ice. Briefly, the minced samples were dissociated using papain and DNase as described [7], always within 2 h of extraction, and maintained overnight in DMEM/F12/N1 base media (composition below), with 20 ng/ml FGF-2 (Sigma Aldrich).

Sorting

The day after dissociation, cells were prepared for either magnetic separation or FACS. PSA-NCAM-defined depletion of cells by magnetic separation was performed as described [9]. CD140a is the same gene as PDGFR alpha in man and the CD140a monoclonal antibody therefore recognizes human PDGFRα [23]. For CD140a or CD9 FACS (BD Pharmingen), cells were re-suspended in PBS with 2mM EDTA and 0.5% BSA and incubated with primary antibody. Isotype and fluorescence-minus one controls were used to set appropriate gates. Each batch of CD140a-PE IgG2a and IgG2a isotype-PE control antibodies (BD Pharmigen) were optimized using flow cytometry, typically over a concentration range of 1:15–1:75. Single cells were discriminated using pulse width and height measurements. After sorting, cells for expression analysis were directly frozen, while cells for in vitro assessment were maintained in a base medium composed of DMEM/F12 (Invitrogen) with HEPES (17.9m), insulin (5 ug/mL), L-glutamine (6.35 mM), D-glucose (46.4 mM), sodium pyruvate (1.5 mM), non-essential amino acids (0.2 mM,), penicillin/streptomycin (40 U/mL), progesterone (57 ng/ml), putrescine (92 μg/ml), selenite (0.065 μg/ml), and transferrin (5mg/mL). For transplantation, cells were maintained in this base medium supplemented with FGF-2 (20 ng/ml) for 1–3 days.

Immunocytochemistry

In culture—Cultures were stained for the early progenitor and oligodendrocyte markers, A2B5 and O4 respectively, as described [5, 13]. Both O4 and A2B5 were localized on live cells that were then fixed with 4% paraformaldehyde. O4 supernatant (gift of R. Bansal and S. Pfeiffer, University of Connecticut) was used at a dilution of 1:100, and monoclonal antibody A2B5 supernatant (clone 105, American Type Culture Collection) was diluted in a 1:1 with DMEM/F12/N1, each was applied for 40 minutes at 4°C. Post-fixation, cultures were stained for astrocyte markers, GFAP (1:1000, Chemicon) and AQP4 (1:200, Chemicon), and for neuronal markers, βIII-tubulin (clone TuJ1, 1:1000, Covance) and HuD (clone 16A11, 10ng/ml, Invitrogen). Oligodendrocyte lineage cells were labeled using Olig2 (1:200, AbCam). Neural progenitor cells were labeled using anti-SOX2 antibody (1:500, R & D Systems). Secondary antibodies, Alexa-488, 594 and 647 conjugated goat-anti mouse IgM, rabbit and rat antibodies respectively were used at a dilution of 1:400 (Invitrogen, La Jolla, CA). Fixed cultures were counterstained with DAPI (10 ng/ml; Invitrogen).

Scoring—The number of phenotypically labeled cells were counted in 10 randomly chosen fields from individual replicate samples (n=3 at each dosage level). Statistical significance was assessed by one-way repeated measures analysis of variance (ANOVA), followed by Dunnett's multiple comparisons test (GraphPad Prism 5, $p<0.05$).

Immunohistochemistry in sections—Transplanted cells were identified using antibody 1281 to human nuclei (1:400, Chemicon), monoclonal antibody 2029 (clone 9.2.27) to human chondroitin sulfate proteoglycan Ng2 (1:200, Chemicon), goat antibody to human Olig2 (1:200, R&D), rabbit antibody 5804 to GFAP (1:1000, Chemicon), rabbit antibody to Ki67 (1:200, LabVision), and rat antibody 7349 to MBP (1:25, Abcam), all as described [7–9, 12]. Confocal imaging was done using an Olympus Fluoview mated to an IX70 inverted microscope, as described. Argon laser lines were used to achieve three-channel immunofluorescence detection of Alexa488-,568- and 647-tagged goat or donkey secondary antibodies (each 1:400, Invitrogen). NG2 immuno-fluorescence was obtained following incubation with biotinylated secondary antibody (1:200, Jackson), and avidin-Alexa488 (1:500, Invitrogen). Three sections at least 350 mm apart were counted (Stereo Investigator, MicroBright Field, Williston,VT), representing rostral, middle, and caudal regions of the fimbria and corpus callosum white matter engraftment for each animal.

Transplantation and tagging

Homozygous shiverer × rag2 immunodeficient mice were bred in our colony. Within 1–2 days of birth, pups were cryoanesthetized for cell delivery. Donor cells (0.5×10^5) in 1 μl of HBSS were injected through a pulled glass pipette and inserted through the skull into the presumptive corpus callosum. Transplants were directed to the corpus callosum at a depth of 1.0–1.2 mm, depending on the weight of the pup, which varied from 1.0 to 1.5 g. Pups were killed at 8 and 12 weeks thereafter. To prevent rejection of xenografts, pups were injected daily with an immunosuppressant FK-506 (5 mg/kg, Tecoland Inc) after reaching 2 weeks of age.

Real-time RT-PCR low density array analyses

Six fetal samples were FACS sorted for CD140a/PDGFRα (21–22 weeks gestational age) and positive and negative fractions collected for molecular analysis. Total RNA was extracted using RNeasy (Qiagen, Chatsworth, CZ) and amplified using ribo-SPIA based whole transcriptome based-amplification (NuGen). The expression of 47 cell type-specific marker genes was assessed using a 48 gene low-density Taqman-based array (TLDA, Applied Biosystems). The complete list of primer probes is given in Supplemental Table 3. The relative abundance of transcript expression was calculated by DDC_t analysis, and the expression data normalized to GAPDH. Genes whose expression was not detected in the more than half of the RNA samples were excluded. Statistical analysis was performed on log_2-transformed data and p-values were corrected for multiple testing using false-discovery rate [38].

Microarray

Extracted total RNA was amplified using 3′-biased ribo-SPIA (NuGen Ovation) and hybridized onto Affymetrix U133+2 arrays according to manufacturer's instructions (Affymetrix). Raw CEL data was processed using RMA [39] and downstream analysis performed using Bioconductor and R [40]. Initial quality control was performed and included measurements of RNA degradation and signal distribution. One sample was removed from further analysis after identification as an outlier following principle component and hierarchical clustering analysis. Genes defined as specifically expressed by PDGFRα$^+$ cells were greater than 3 fold expressed and significant using a moderated t-test statistic with 5% false discovery rate cut-off ($q<0.05$, n=5; linear modeling empirical Bayes test statistic)[41]. The differentially expressed genes were further filtered to removed genes highly expressed by human microglial cells (CD11b-defined, n=3), relative to adult A2B5-sorted OPCs [13]. Gene ontology and Ingenuity Pathway Analysis were performed on the list of PDGFRα specific genes. Gene ontology over-representation was performed using NIH DAVID[42]. Significance p-values calculated in Ingenuity were based on a right-tailed Fisher's Exact test to identify over-represented functional/pathway annotations, that is annotations which have more differentially expressed genes than expected by chance. Individual networks of interesting genes were selected according to relevance score and composition of gene constituents. Gene set enrichment analysis was performed using the PGSEA package [43] and significance assessed by fitting the relative enrichment of individual pathways to a linear model and using a moderated t-test statistic to assign significance. The resulting p-values were corrected for multiple testing correction using the false discovery rate. The complete microarray dataset is available at GEO under the accession no. GSE29368.

Supplementary Material

Refer to Web version on PubMed Central for supplementary material.

Acknowledgments

This work was supported by NINDS R01NS039559, the Adelson Medical Research Foundation, the Mathers Charitable Foundation, the National Multiple Sclerosis Society, and the New York State Stem Cell Research Board

(NYSTEM). We would like to thank Xiao-Jie Li for technical support, and Michelle Zanche, Andrew Cardillo and the URMC Functional Genomics core for Affymetrix and Taqman array support.

References

1. Ben-Hur T, Goldman SA. Prospects of cell therapy for disorders of myelin. Ann N Y Acad Sci. 2008; 1142:218–249. [PubMed: 18990129]
2. Franklin RJ, Ffrench-Constant C. Remyelination in the CNS: from biology to therapy. Nat Rev Neurosci. 2008; 9:839–855. [PubMed: 18931697]
3. Goldman SA. Progenitor cell-based treatment of the pediatric myelin disorders. Archives of Neurology. 2011; 68:848–856. [PubMed: 21403006]
4. Scolding N, et al. Oligodendrocyte progenitors are present in the normal adult human CNS and in the lesions of multiple sclerosis. Brain. 1998; 121:2221–2228. [PubMed: 9874475]
5. Roy NS, et al. Identification, isolation, and promoter-defined separation of mitotic oligodendrrocyte progenitor cells from the adult human subcortical white matter. J Neurosci. 1999; 19:9986–9995. [PubMed: 10559406]
6. Scolding N. Glial precursor cells in the adult human brain. Neuroscientist. 1998; 4:264–272.
7. Windrem MS, et al. Fetal and adult human oligodendrocyte progenitor cell isolates myelinate the congenitally dysmyelinated brain. Nature Medicine. 2004; 10:93–97.
8. Windrem MS, et al. Progenitor cells derived from the adult human subcortical white matter disperse and differentiate as oligodendrocytes within demyelinated lesions of the rat brain. J Neurosci Res. 2002; 69:966–975. [PubMed: 12205690]
9. Windrem MS, et al. Neonatal chimerization with human glial progenitor cells can both remyelinate and rescue the otherwise lethally hypomyelinated shiverer mouse. Cell Stem Cell. 2008; 2:553–565. [PubMed: 18522848]
10. Eisenbarth GS, Walsh FS, Nirenberg M. Monoclonal antibody to a plasma membrane antigen of neurons. Proc Natl Acad Sci U S A. 1979; 76:4913–4917. [PubMed: 388422]
11. Raff MC, Miller RH, Noble M. A glial progenitor cell that develops in vitro into an astrocyte or an oligodendrocyte depending on culture medium. Nature. 1983; 303:390–396. [PubMed: 6304520]
12. Nunes MC, et al. Identification and isolation of multipotential neural progenitor cells from the subcortical white matter of the adult human brain. Nature Medicine. 2003; 9:439–447.
13. Sim F, et al. Complementary patterns of gene expression by adult human oligodendrocyte progenitor cells and their white matter environment. Ann Neurology. 2006; 59:763–779.
14. Belachew S, et al. Postnatal NG2 proteoglycan-expressing progenitor cells are intrinsically multipotent and generate functional neurons. Journal of Cell Biology. 2003; 161:169–186. [PubMed: 12682089]
15. Cahoy JD, et al. A transcriptome database for astrocytes, neurons, and oligodendrocytes: a new resource for understanding brain development and function. J Neurosci. 2008; 28:264–278. [PubMed: 18171944]
16. Pringle NP, Mudhar HS, Collarini EJ, Richardson WD. PDGF receptors in the rat CNS: during late neurogenesis, PDGF alpha- receptor expression appears to be restricted to glial cells of the oligodendrocyte lineage. Development. 1992; 115:535–551. [PubMed: 1425339]
17. Nishiyama A, Lin XH, Giese N, Heldin CH, Stallcup WB. Co-localization of NG2 proteoglycan and PDGF alpha-receptor on O2A progenitor cells in the developing rat brain. J Neurosci Res. 1996; 43:299–314. [PubMed: 8714519]
18. Ellison JA, de Vellis J. Platelet-derived growth factor receptor is expressed by cells in the early oligodendrocyte lineage. J Neurosci Res. 1994; 37:116–128. [PubMed: 8145299]
19. Gogate N, et al. Plasticity in the adult human oligodendrocyte lineage. J Neurosci. 1994; 14:4571–4587. [PubMed: 7519254]
20. Zhang SC, Ge B, Duncan ID. Tracing human oligodendroglial development in vitro. J Neurosci Res. 2000; 59:421–429. [PubMed: 10679779]
21. Berry M, Hubbard P, Butt AM. Cytology and lineage of NG2-positive glia. J Neurocytology. 2002; 31:457–467.

22. Terada N, et al. Then tetraspanin protein CD9 is expressed by progenitor cells committed to oligodendrogenesis and is linked to B1 integrin CD81 and Tspan2. Glia. 2002; 40:350–359. [PubMed: 12420314]
23. LaRochelle WJ, et al. Inhibition of platelet-derived growth factor autocrine growth stimulation by a monoclonal antibody to the human alpha platelet-derived growth factor receptor. Cell Growth Differ. 1993; 4:547–553. [PubMed: 7691151]
24. Chang A, Nishiyama A, Peterson J, Prineas J, Trapp BD. NG2-positive oligodendrocyte progenitor cells in adult human brain and multiple sclerosis lesions. J Neurosci. 2000; 20:6404–6412. [PubMed: 10964946]
25. Kirschenbaum B, et al. In vitro neuronal production and differentiation by precursor cells derived from the adult human forebrain. Cerebral Cortex. 1994; 4:576–589. [PubMed: 7703685]
26. Armstrong RC, Dorn HH, Kufta CV, Friedman E, Dubois-Dalcq ME. Pre-oligodendrocytes from adult human CNS. J Neurosci. 1992; 12:1538–1547. [PubMed: 1556607]
27. Wegner M, Stolt CC. From stem cells to neurons and glia: a Soxist's view of neural development. Trends Neurosci. 2005; 28:583–588. [PubMed: 16139372]
28. Wang S, et al. Prospective identification, isolation, and profiling of a telomerase-expressing subpopulation of human neural stem cells, using sox2 enhancer-directed fluorescence-activated cell sorting. J Neurosci. 2010; 30:14635–14648. [PubMed: 21048121]
29. Rakic S, Zecevic N. Early oligodendrocyte progenitor cells in the human fetal telencephalon. Glia. 2003; 41:117–127. [PubMed: 12509802]
30. Back SA, et al. Late oligodendrocyte progenitors coincide with the developmental window of vulnerability for human perinatal white matter injury. J Neurosci. 2001; 21:1302–1312. [PubMed: 11160401]
31. Noble M, Murray K, Stroobant P, Waterfield MD, Riddle P. Platelet-derived growth factor promotes division and motility and inhibits premature differentiation of the oligodendrocyte/type-2 astrocyte progenitor cell. Nature. 1988; 333:560–562. [PubMed: 3287176]
32. Wolswijk G, Noble M. Cooperation between PDGF and FGF converts slowly dividing O-2A adult progenitor cells to rapidly dividing cells with characteristics of O-2Aperinatal progenitor cells. J Cell Biol. 1992; 118:889–900. [PubMed: 1323567]
33. Mabie PC, et al. Bone morphogenetic proteins induce astroglial differentiation of oligodendroglial-astroglial progenitor cells. J Neurosci. 1997; 17:4112–4120. [PubMed: 9151728]
34. Lillien LE, Raff MC. Analysis of the cell-cell interactions that control type-2 astrocyte development in vitro. Neuron. 1990; 4:525–534. [PubMed: 2182078]
35. Keyoung HM, Goldman SA. Glial progenitor-based repair of demyelinating neurological diseases. Neurosurg Clin NA. 2007; 18:93–104.
36. Meng K, et al. Pleiotrophin signals increased tyrosine phosphorylation of beta beta-catenin through inactivation of the intrinsic catalytic activity of the receptor-type protein tyrosine phosphatase beta/zeta. 2000; 97:2603–2608.
37. Fancy SP, et al. Dysregulation of the Wnt pathway inhibits timely myelination and remyelination in the mammalian CNS. Genes Dev. 2009; 23:1571–1585. [PubMed: 19515974]
38. Hochberg Y, Benjamini Y. More powerful procedures for multiple significance testing. Stat Med. 1990; 9:811–818. [PubMed: 2218183]
39. Irizarry RA, et al. Exploration, normalization, and summaries of high density oligonucleotide array probe level data. Biostatistics. 2003; 4:249–264. [PubMed: 12925520]
40. Gentleman R, et al. Bioconductor: open software development for computational biology and bioinformatics. Genome Biol. 2004; 5:R80. [PubMed: 15461798]
41. Smyth G. Linear models and empirical bayes methods for assessing differential expression in microarray experiments. Stat Appl Genet Mol Biol. 2004; 3:Article 3.
42. Dennis G Jr, et al. Integrated Discovery. Genome Biol. 2003; 4:P3. [PubMed: 12734009]
43. Furge, K.; Dykema, K., editors. R package 1.10.0 R package. 2006.

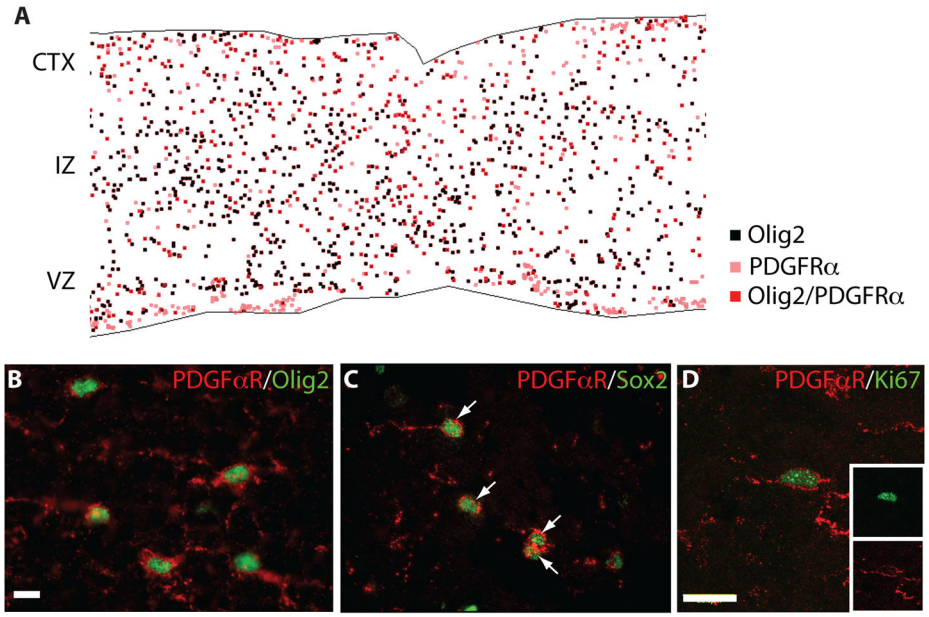

Figure 1. CD140a identifies a proliferating oligodendrocyte progenitor in fetal cortex and intermediate zone

CD140a/PDGFRα$^+$ cells were found in the cortical mantle of 22 wk gestational age (g.a.) human fetal brain. **A,** All identifiable CD140a$^+$ cell bodies co-expressed the oligodendrocyte lineage transcription factor Olig2. **B,** Consistent with an early neural progenitor phenotype, CD140a$^+$/PDGFRα$^+$ cells within the intermediate zone co-expressed the progenitor-expressed transcription factor sox2. **C,** A proportion of PDGFRα$^+$/CD140a$^+$ cells co-labeled with Ki67 antibody, a marker of cells in active cell cycle. The main panel shows a confocal z-stack (CD140a, *red*; Ki67, *green*); the *inset* shows fluorophore-specific single optical sections of the imaged cell. **D,** shows a low power schematic reconstruction of the distribution of CD140a/PDGFRα-immunoreactive cells in a section of 18 week forebrain, showing the broad dispersal of these cells through the intermediate zone and cortical mantle. Scale: **A–C**, 20 μm; **D**, 1 mm.

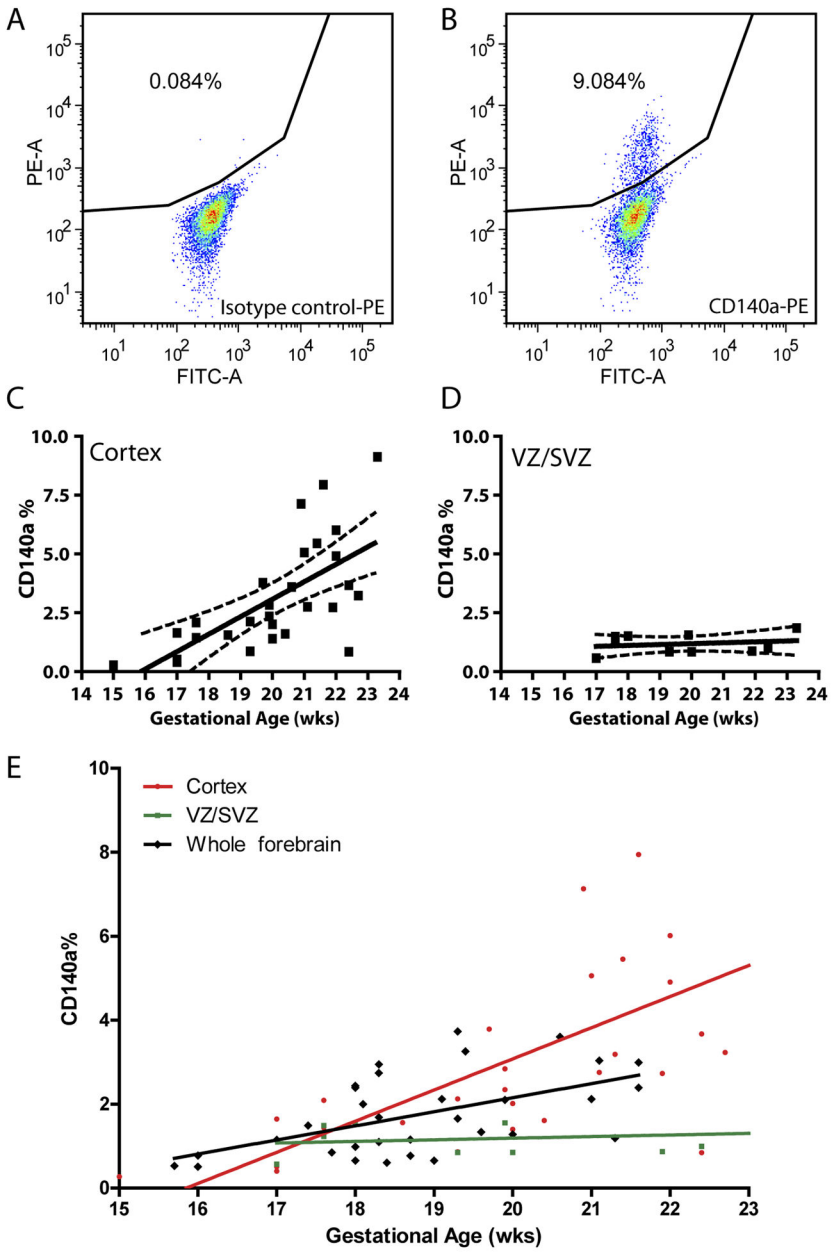

Figure 2. CD140a/PDGFRα recognizes a population of cells in the fetal brain that accumulate with gestational age in the intermediate zone and cortex

Flow cytometry was used to determine the relative abundance of PDGFRα$^+$ cells in the fetal human germinal zones and overlying intermediate zone and cortex. A, B, shows a typical CD140a cytometry of a 21 wk fetal cortical/IZ dissociate. A, shows limited non-specific staining using a PE-conjugated isotype control; B, the same dissociate stained using PE-conjugated anti-CD140a. CD140a$^+$ cells were uncommon in the second trimester intermediate zone and cortex before 16 weeks g.a.; their incidence increased thereafter with gestational age (n=29) (C). In contrast, the incidence of CD140a$^+$ cells remained relatively constant throughout the second trimester in the VZ/SVZ (n=10) (D). E shows a

superimposition of all CD140a incidence data, as multiple regression lines including whole forebrain as well as dissected VZ/SVZ and IZ/cortex.

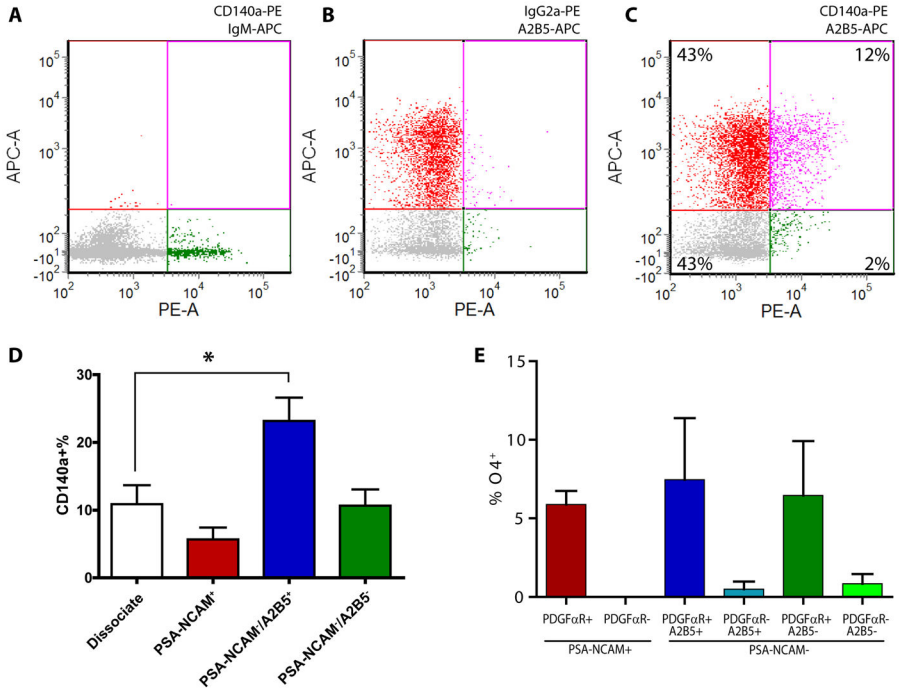

Figure 3. CD140a/A2B5/PSA-NCAM cytometry

Fetal dissociates were immunomagnetically selected on the basis of PSA-NCAM antigenicity. PSA-NCAM$^-$ cells were then subject to two-color FACS for CD140a and A2B5 using PE- and APC-conjugated antibodies, respectively (**A–C**). Positive selection gates were defined using fluorescence-minus one (FMO) controls by substitution of either A2B5 (**A**) or CD140a (**B**) antibodies with a matched isotype control conjugated antibody. A2B5 and C140a-specific antibodies were combined in **C**. A large proportion of CD140a$^+$ cells co-expressed A2B5 (**C**). PSA-NCAM$^+$ cell underwent single color CD140a cytometry/ FACS (not shown). **D,** shows the proportion of CD140a$^+$ cells in each A2B5/PSA-NCAM sorted fractions (n=4, 19–22wk gestational age). The A2B5$^+$PSA-NCAM$^-$ fraction contained significantly more CD140a$^+$ cells than unsorted dissociate (1-way ANOVA followed by Dunnett's multiple comparison test, $p<0.05$). **E,** each sorted fraction was cultured in T3/0.5% PD-FBS media for 7 days and assessed for the immature oligodendrocyte antigen O4. CD140a$^+$ cells from each A2B5/PSA-NCAM fraction gave rise to a higher proportion of O4$^+$ oligodendrocytes than matched CD140a$^-$cells (n=3 samples).

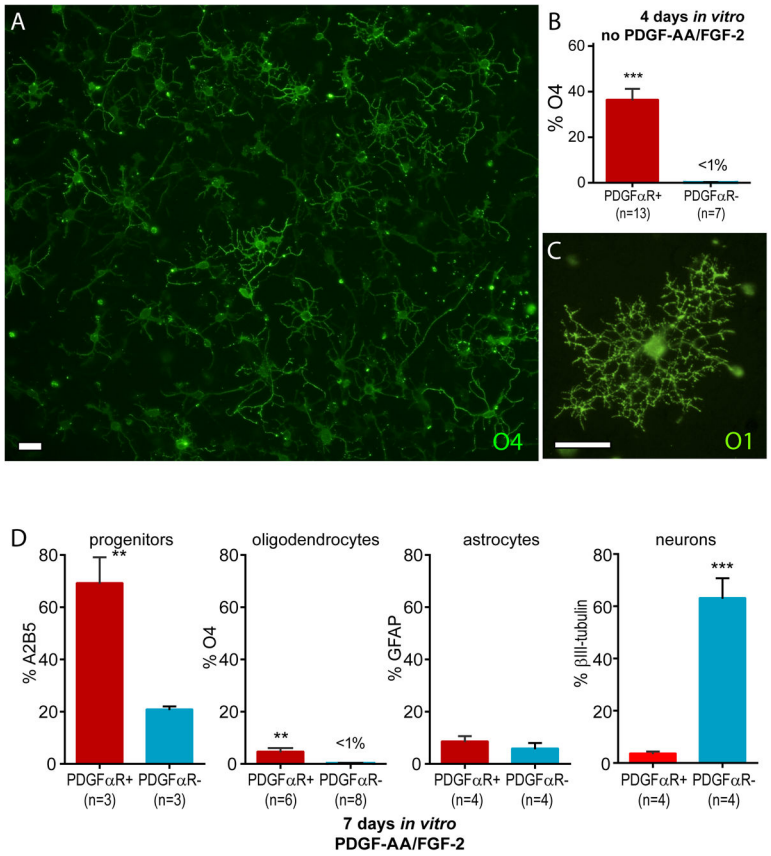

Figure 4. CD140a-sorted cells mature primarily as oligodendrocytes but can be maintained as bipotential progenitors

Sorted CD140a$^+$ cells were plated onto substrate and allowed to differentiate following removal of exogenous growth factors. **A**, by 4 days after FACS, these cells had developed characteristic immature oligodendrocyte morphology expressing the sulfatide antigen O4. The proportion of O4$^+$ oligodendrocytes was determined at 4 days in vitro (**B**). Virtually no O4-defined oligodendrocytes were found in CD140a-depleted cultures; in contrast, approximately 40% of CD140a$^+$ cells developed O4 expression by that point. **C**, 7 days post-sort some oligodendrocytes had matured further with elaborate oligodendrocyte profiles stained with O1 antibody. **D**, CD140a-sorted cells were cultured for 7 days in the presence of PDGF-AA and FGF-2 (20 ng/ml each), then immunophenotyped. Under these conditions, CD140a$^+$ cells continued to express A2B5, while less than 10% developed O4$^+$ expression. In contrast, the CD140a$^-$ fraction was comprised primarily of βIII-tubulin$^+$ neurons. Scale = 10 μm.

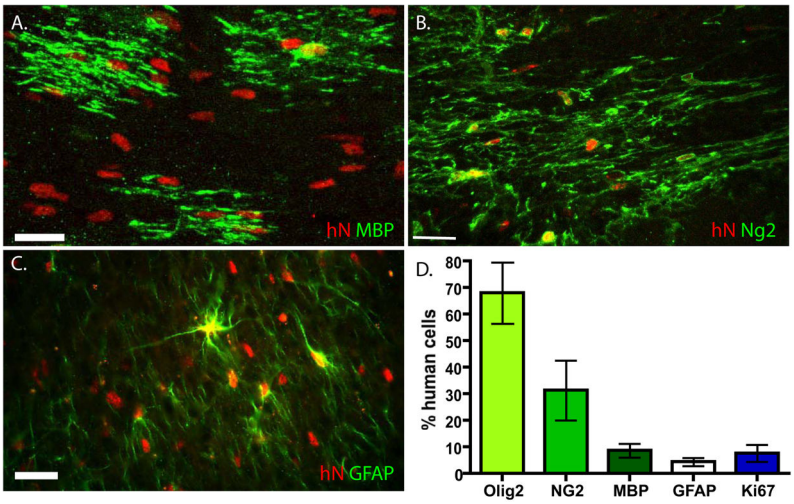

Figure 5. CD140a sorted cells can efficiently myelinate shiverer axons

Human fetal CD140a$^{+/}$PDGFRα^{+} OPCs were transplanted into the hypomyelinated forebrain of neonatal, rag2 null-immunodeficient *shiverer* mice. At 8 weeks post injection, a fraction of human cells recognized by anti-human nuclear antigen (hNA, *red*) differentiated into myelinating oligodendrocytes expressing the myelin protein gene MBP (*green*) (**A**). Consistent with the time course of human myelination, a large proportion of transplanted CD140a^{+} cells remained as NG2-expressing OPCs at 8 weeks post-implantation (**B**), while a minor fraction differentiated as astrocytes, as immunolabeled by GFAP (**C**). **D** illustrates a quantification of human CD140a^{+} cell fate, at 8 weeks post implantation (n=3). Scale = 20 μm.

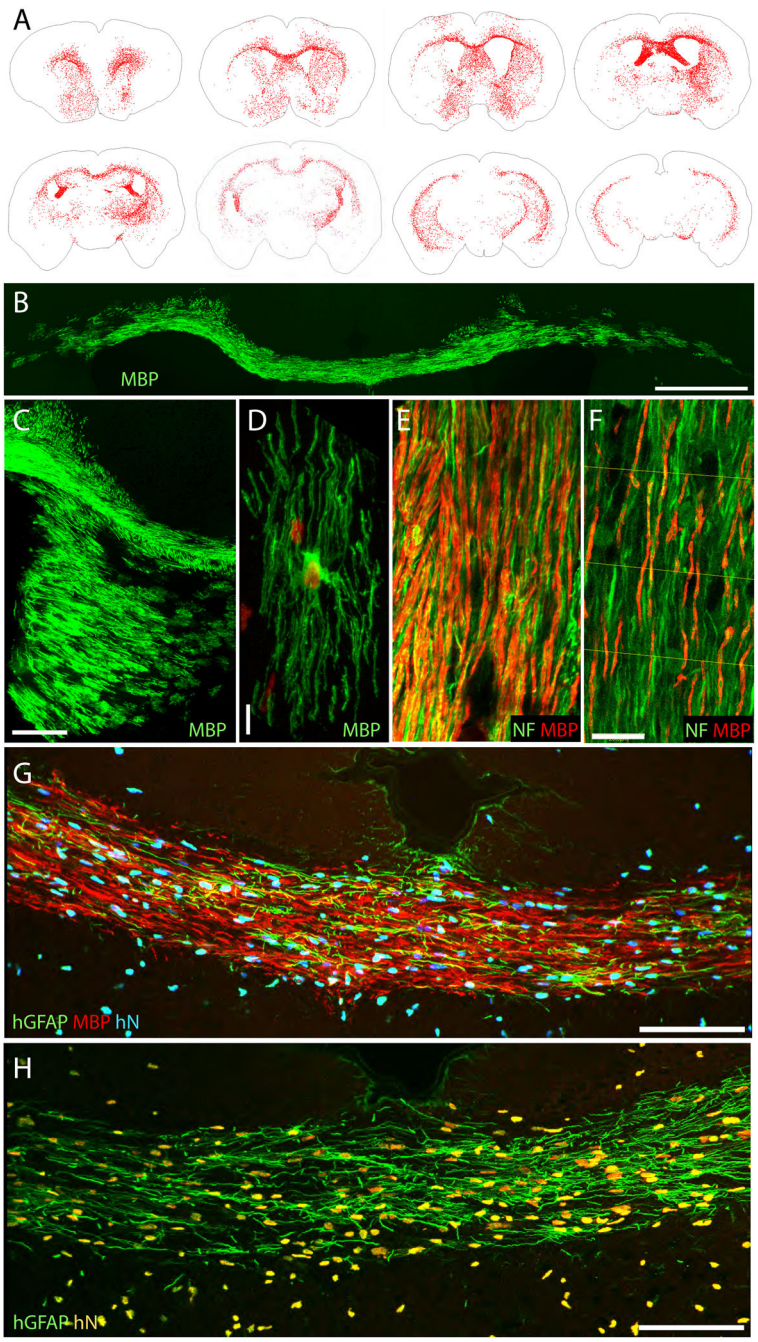

Figure 6. CD140a-sorted OPCs myelinate more effectively than A2B5-sorted OPCs

A, Computer-assisted drawings of 14 μm sections taken at 0.67 mm intervals throughout the forebrain of a 12 week old shiverer × rag2-null mouse, transplanted bilaterally in the corpus callosum with 100,000 cells sorted on CD140a/PDGFRα. Each red dot represents an individual cell labeled with anti-human nuclear antigen. **B,** The corpus callosum of an engrafted shiverer mouse at 12 weeks, stained for myelin basic protein (MBP, *green*), showing substantial donor-derived myelin. **C,** A photomicrograph of the corpus callosum and fimbria in another engrafted mouse; MBP, *green*. **D**, An individual oligodendrocyte,

stained for anti-human nuclear antigen (*red*) and MBP (*green*). **E–F,** Ensheathment of host mouse axons (neurofilament, *green*; MBP, *red*) at 12 weeks by human fetal cells sorted on the basis of either CD140a/PDGFRα(**E**) or A2B5-immunoreactivity (**F**), manifesting the more rapid and robust axonal myelination by $CD140a^+$ cells than by A2B5-sorted cells. **G–H,** Sections of a CD140a-engrafted shiverer callosum at 12 weeks, immunostained for MBP (*red*), human GFAP (*green*), and human nuclear antigen (*blue* in **G**, *yellow* in **H**). These images show the robust production of $hGFAP^+$ astrocytes as well as MBP^+ oligodendrocytes from the engrafted $CD140a^+$ cells in vivo.
Scale: **B**, 500 μm; **C**, 200 μm; **D**, 10 μm; **E–F**, 20 μm.

Table 1

Marker gene expression by CD140a$^+$/PDGFRα$^+$ fetal human oligodendrocyte progenitors

Fetal cortical dissociates were FACS sorted for CD140a/PDGFRa immunoreactivity and immediately frozen for RNA analysis (n=6 fetal samples). Expression of cell type-specific markers was measured by quantitative Taqman RT-PCR and compared against the matched CD140a$^-$/PDGFRα$^-$ pool. Expression data was calculated via normalization to GAPDH, and significance was assessed by paired *t*-test statistics. P-value were adjusted for multiple testing effects using false discovery rate (q-value). Mean ratio of expression and standard error ranges are shown. Significantly expressed genes at 5% FDR are bolded; significantly depleted genes are *italicized*. OPC-expressed genes were highly enriched in fetal CD140a/PDGFRα-sorted cells.

Cell Type	Symbol (Name)	qPCR ratio
Oligodendrocyte progenitor	CSPG4 (NG2)	47.95 (14.73 – 156.04)
	PDGFRA	**524.65 (175.68 – 1,566.81; q =0.021)**
	PTPRZ1 (RPTPzeta)	**3.74 (2.81 – 4.99; q =0.034)**
	GD3 synthase	1.43 (0.91 – 2.23)
Oligodendrocyte lineage	**CNP**	**4.89 (3.83 – 6.24; q =0.020)**
	Nkx2.2	**42.83 (17.36 – 105.66; q =0.042)**
	Olig1	**54.79 (28.14 – 106.67; q =0.021)**
	Olig2	**196.05 (92.19 – 416.91; q =0.020)**
	SOX10	**578.59 (247.93 – 1,350.21; q =0.020)**
Myelinating oligodendrocyte	**CLDN11 (claudin 11/OTP)**	**16.64 (8.27 – 33.47; q =0.042)**
	GALC	1.06 (0.87 – 1.29)
	MBP	1.25 (0.22 – 7.20)
	MOBP	0.52 (0.11 – 2.47)
	MOG	0.10 (0.04 – 0.25)
	NKX6.2 (Gtx)	6.29 (1.71 – 23.08)
	PLP1 (PLP/DM20)	1.30 (0.78 – 2.16)
Astrocyte	AQP4	0.79 (0.59 – 1.07)
	GFAP	3.83 (1.94 – 7.56)
	GLUL (glutamine synthase)	4.94 (2.28 – 10.71)
	S100B	**69.52 (23.10 – 209.17; q =0.046)**
	SLC1A2 (GLT-1)	1.09 (0.99 – 1.20)
	TNC (tenascin C)	2.12 (1.58 – 2.85)
	CD44	2.89 (2.07 – 4.05)
Radial Glia	FABP7 (BLBP)	1.58 (1.30 – 1.93)
	SLC1A3 (GLAST)	2.53 (1.88 – 3.41)
Neural progenitor and stem cell	ASCL1 (MASH1)	1.68 (1.12 – 2.50)
	DCX (doublecortin)	*0.28 (0.20 – 0.39; q =0.046)*
	SOX1	0.64 (0.38 – 1.09)
	HES1	3.40 (1.88 – 6.13)

Cell Type	Symbol (Name)	qPCR ratio
	MSI1	*0.37 (0.28 – 0.48; q =0.046)*
	NES	2.23 (1.64 – 3.04)
	NR2E1 (tailless)	0.43 (0.23 – 0.83)
	SOX2	**4.52 (2.96 – 6.88; q =0.046)**
Neuron	MAP2	1.20 (0.88 – 1.64)
	NEFH	0.42 (0.29 – 0.61)
	TUBA1A (T alpha 1)	*0.37 (0.29 – 0.49; q =0.046)*
	TUBB3 (βIII-tubulin)	*0.31 (0.23 – 0.41; q =0.042)*
	ELAVL3 (HuC)	0.51 (0.37 – 0.70)
	ELAVL4 (HuD)	*0.21 (0.15 – 0.29; q =0.034)*
Endothelial	CDH5 (VE-cadherin)	0.56 (0.37 – 0.86)
	TEK (TIE2)	1.90 (1.29 – 2.80)
	VWF	0.50 (0.11 – 2.33)
Microglial	**CD68**	**3.41 (2.41 – 4.84; q =0.046)**
	CD86	**78.63 (32.96 – 187.57; q =0.031)**
	PTPRC (LCA)	25.19 (9.05 – 70.08)